Volume 9
Number 7
7 April 2025
Pages 1607–1906

Sustainable Energy & Fuels

Interdisciplinary research for the development of sustainable energy technologies

rsc.li/sustainable-energy

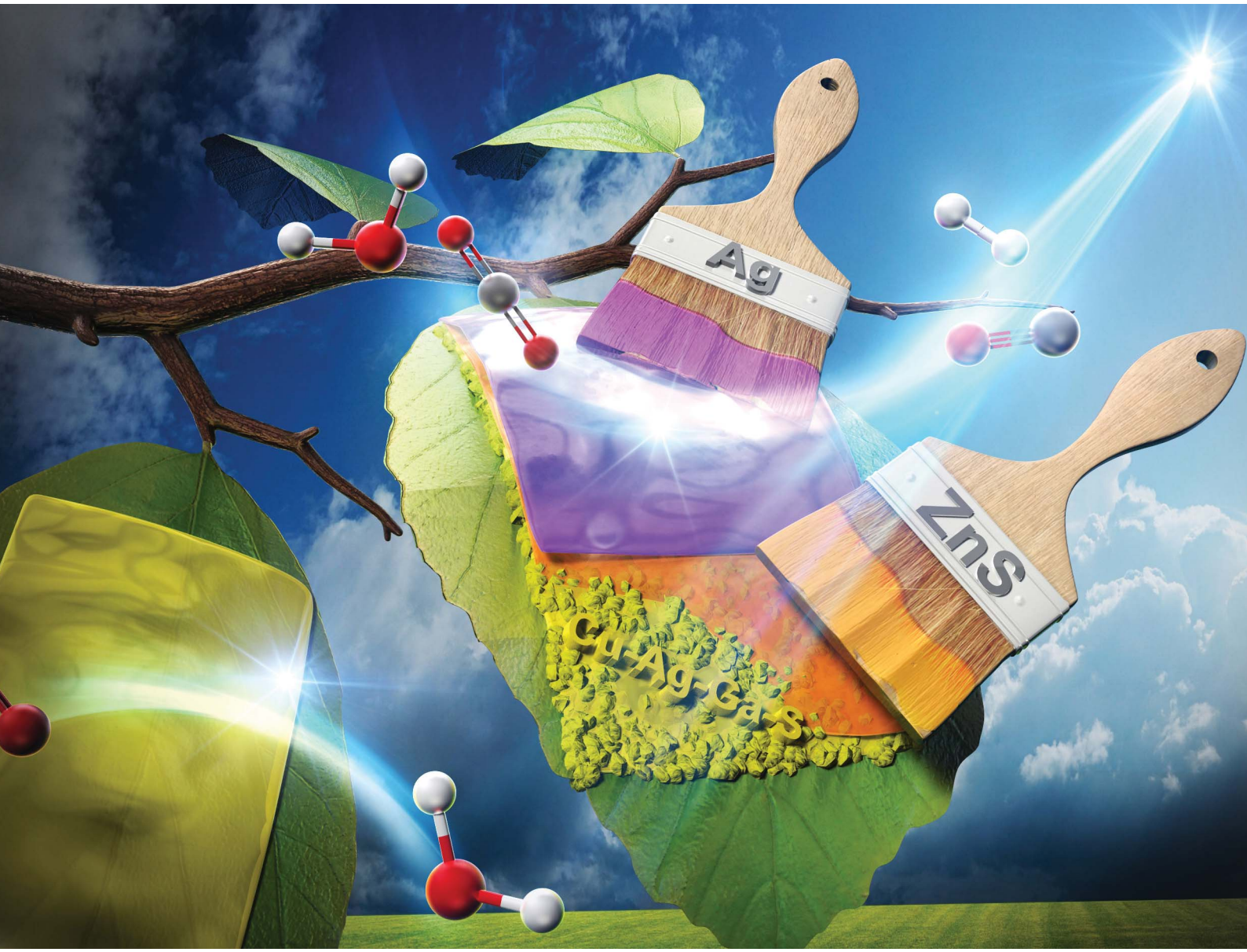

ISSN 2398-4902

ROYAL SOCIETY OF CHEMISTRY

PAPER

Akihiko Kudo *et al.*

Improvement of performance to form syngas utilizing water and CO_2 over a particulate-$Cu_{0.8}Ag_{0.2}GaS_2$-based photocathode by surface co-modification with ZnS and Ag

Sustainable Energy & Fuels

ROYAL SOCIETY OF CHEMISTRY

PAPER

View Article Online
View Journal | View Issue

Check for updates

Cite this: *Sustainable Energy Fuels*, 2025, 9, 1709

Improvement of performance to form syngas utilizing water and CO_2 over a particulate-$Cu_{0.8}Ag_{0.2}GaS_2$-based photocathode by surface co-modification with ZnS and Ag†

Tomoaki Takayama, ‡[a] Akihide Iwase §[a] and Akihiko Kudo *[ab]

Received 12th December 2024
Accepted 23rd January 2025

DOI: 10.1039/d4se01738b

rsc.li/sustainable-energy

Surface of a particulate-$Cu_{0.8}Ag_{0.2}GaS_2$-based photocathode was co-modified with ZnS and Ag, resulting in improvement in the performance of the $Cu_{0.8}Ag_{0.2}GaS_2$ photocathode for syngas (H_2 + CO) formation through photoelectrochemical H_2O and CO_2 reduction under visible light in an aqueous electrolyte. Bubbles of the syngas were visually observed over the developed Ag and ZnS-co-modified $Cu_{0.8}Ag_{0.2}GaS_2$ photocathode at 0 V *vs.* RHE at the applied potential using a 300 W Xe-arc lamp (λ > 420 nm). Based on various control experiments and characterization studies, the following two crucial factors have arisen: (1) formation of a (ZnS)–($Cu_{0.8}Ag_{0.2}GaS_2$) solid-solution near the surface of $Cu_{0.8}Ag_{0.2}GaS_2$ particles was vital for enhancing the separation of the photogenerated carriers, (2) the Ag cocatalyst loaded on the solid-solution worked as an active site for photoelectrochemical CO_2 reduction. Moreover, artificial photosynthetic syngas formation using water as an electron donor under simulated sunlight without any external bias was demonstrated by combining the developed Ag/ZnS/$Cu_{0.8}Ag_{0.2}GaS_2$ photocathode with a CoO_x-loaded $BiVO_4$ photoanode.

Open Access Article. Published on 27 January 2025. Downloaded on 2/13/2026 6:04:03 AM.
This article is licensed under a Creative Commons Attribution-NonCommercial 3.0 Unported Licence.

1 Introduction

Photoelectrochemical systems which consist of a photocathode and a photoanode have been extensively studied not only for water splitting[1,2] but also for CO_2 reduction[3–5] using water as an electron donor. This is because these systems possess a potential to produce H_2 and CO as reduction products of water and CO_2 separately from O_2 as an oxidation product of water. The mixture of H_2 and CO is called syngas that can be used as a raw chemical for liquid fuels, lower olefines and aromatics synthesis.[6] In this context, it is important to explore highly active photocathodes for syngas formation in terms of utilization of CO_2 and solar energy.

From the viewpoint of the construction of highly efficient photoelectrochemical cells,[1,7] metal sulfide photocathodes are attractive because of their narrow band gaps and positive onset potentials for the cathodic photocurrent.[8] In particular, particulate-metal-sulfide-based photocathodes are advantageous because they can easily be fabricated as compared with a thin film photocathode using a vacuum process. We have reported that a particulate solid-solution of $CuGaS_2$ and $AgGaS_2$ (*e.g.*, $Cu_{0.8}Ag_{0.2}GaS_2$) provides higher photocathodic performance than that of pristine $CuGaS_2$ in photoelectrochemical water reduction to form hydrogen under visible light.[9] Moreover, the report[10] that a particulate-$(CuGa)_{0.5}ZnS_2$-based photocathode is active for syngas formation under visible light motivated us to use a particulate-$Cu_{0.8}Ag_{0.2}GaS_2$-based photocathode for syngas formation. However, the photoelectrochemical performance of such a particulate-based photocathode is generally not yet enough to build photoelectrochemical cells that work under solar light if modifications such as loading cocatalysts are not performed. Therefore, it is important to discover a surface modification method being effective for improving the performance of $Cu_{0.8}Ag_{0.2}GaS_2$ in order to apply $Cu_{0.8}Ag_{0.2}GaS_2$ to a photocathode for syngas formation utilizing water and CO_2 under sunlight.

Various surface modifications of photocathodes have been investigated to develop highly active photocathodes. To date, Cu_2ZnSnS_4,[11,12] Cu_2ZnGeS_4,[13] $CuInS_2$,[14] Cu(In,Ga)Se_2,[15] *p*-InP,[16,17] *p*-ZnTe,[18] *p*-Si,[19,20] N-doped Ta_2O_5,[16] $CuFeO_2$,[21] Cu_2O,[22] $CuGaO_2$,[23] and *p*-Fe_2O_3 (ref. 24) have emerged to showcase their performances for CO_2 reduction to form CO and HCOOH in aqueous solutions under visible light irradiation, which have been

[a]*Department of Applied Chemistry, Faculty of Science, Tokyo University of Science, 1-3 Kagurazaka, Shinjuku-ku, Tokyo 162-8601, Japan. E-mail: a-kudo@rs.tus.ac.jp*

[b]*Research Institute of Science and Technology, Carbon Value Research Center, Tokyo University of Science, Noda-shi, Chiba-ken 278-8510, Japan*

† Electronic supplementary information (ESI) available: X-ray photoelectron spectroscopic measurements. See DOI: https://doi.org/10.1039/d4se01738b

‡ Present address: His current affiliation is Graduate School of Science and Technology, Division of Materials Science, Nara Institute of Science and Technology, 8916-5 Takayama, Ikoma, Nara 630-0192, Japan.

§ Present address: His current affiliation is Department of Applied Chemistry, School of Science and Technology, Meiji University, Kanagawa 214-8571, Japan.

Open Access Article. Published on 27 January 2025. Downloaded on 2/13/2026 6:04:03 AM. This article is licensed under a Creative Commons Attribution-NonCommercial 3.0 Unported Licence.

improved by surface modifications. Specifically, n-type semiconductors, metal complexes, or metal nanoparticles have been investigated as the modifications. Furthermore, judging from the progress in photoelectrochemical water splitting,[1,8] co-modification of metal sulfide photocathodes with n-type semiconductors and metallic cocatalysts is expected to bring highly efficient photocathodes for CO_2 reduction. This is because co-modifications with n-type semiconductors and noble cocatalysts are frequently employed to enhance the separation of photogenerated electron–hole pairs and introduce active sites for water reduction.

Herein, we focused on the combination of ZnS with metallic cocatalysts as a co-modification. This is because ZnS is an n-type semiconductor being effective in improvement of syngas formation on the Cu_2ZnGeS_4 thin film photocathode[13] of which the crystal structure is similar to the chalcopyrite structure of $Cu_{0.8}Ag_{0.2}GaS_2$. ZnS is expected to be easily formed on the surfaces of particulate-metal-sulfide-based photocathodes by a chemical deposition method.[25] Additionally, the toxicity of ZnS is lower than that of CdS, which is another typical n-type semiconductor. We first investigated the effects of modification conditions to deposit ZnS over particulate-$Cu_{0.8}Ag_{0.2}GaS_2$-based photocathodes on their photocathodic performances for CO_2 reduction. Sequentially, we investigated additional modifications of the ZnS-modified photocathodes with various cocatalysts. Then, we discovered a co-modification for fabricating an active photocathode for CO_2 reduction to form syngas under simulated solar light, resulting in artificial photosynthetic syngas formation upon combining the developed photocathode with a CoO_x-loaded $BiVO_4$ photoanode.

2 Experimental methods

2.1 Preparation and characterization of a particulate-$Cu_{0.8}Ag_{0.2}GaS_2$-based photocathode

A particulate $Cu_{0.8}Ag_{0.2}GaS_2$ photocatalyst was prepared by a solid-state reaction according to a previous report.[9] Starting materials Cu_2S (Kojundo; 99%), Ag_2S (Rare Metallic; 99.9%), and Ga_2S_3 (Kojundo; 99.99%) were ground using an agate mortar. A 10% excess amount of Ga_2S_3 was added to the starting materials. This Ga_2S_3-rich condition is effective in improving performance of $Cu_{0.8}Ag_{0.2}GaS_2$.[9] The mixture sealed in a quartz ampoule tube after evacuation (<0.1 Pa) was heated at 1073 K for 10 h to obtain $Cu_{0.8}Ag_{0.2}GaS_2$ powder. The obtained powder was identified to be an almost single-phase by powder X-ray diffraction (Rigaku; Miniflex, X-ray source; Cu Kα). Diffuse reflectance spectra of powder and photocathode samples were obtained using a UV-vis-NIR spectrometer (Jasco; UbestV-570) with an integrating sphere, and were converted to absorbance spectra from the reflection by the Kubelka–Munk function. As the reference samples, $(ZnS)_{2x}$–$(Cu_{0.8}Ag_{0.2}GaS_2)_x$ solid-solutions were prepared by the same procedure above. ZnS (Sigma-Aldrich, 99.99%) was used as the starting material.

A pristine particulate-$Cu_{0.8}Ag_{0.2}GaS_2$-based photocathode was prepared by a drop-casting method. The $Cu_{0.8}Ag_{0.2}GaS_2$ powder was dispersed in ethanol (2–8 mg mL^{-1}). This suspension was dripped on a FTO substrate (Asahi Glass; F-doped SnO_2) and thereby $Cu_{0.8}Ag_{0.2}GaS_2$ powder was accumulated on the substrate with 5 mg cm^{-2}. After drying up the ethanol at room temperature, the accumulated powder was annealed at 773 K for 2 h in N_2 gas to obtain a pristine particulate-$Cu_{0.8}Ag_{0.2}GaS_2$-based photocathode.

Modification of the pristine particulate-$Cu_{0.8}Ag_{0.2}GaS_2$-based photocathode (denoted as CAGS) with ZnS was conducted by a chemical bath deposition method according to the literature.[25] The notation of the photocathodes prepared under different conditions is summarized in Table 1. The detailed procedures of the experiments are explained as follows. $ZnSO_4 \cdot 7H_2O$ (Wako; 99.5%), thiourea (Wako; 98.0%) and citric acid (Wako; 98.0%) employed as the starting materials were dissolved in 270 mL of water at 353 K at concentrations of 0.033, 0.066 and 0.088 mol L^{-1}, respectively. After adding 30 mL of 25% of an aqueous ammonia solution (Wako) into the aqueous solution, a pristine particulate-$Cu_{0.8}Ag_{0.2}GaS_2$-based photocathode was immediately immersed into the final mixture for 10 minutes to deposit ZnS on the surface of the pristine photocathode. The ZnS-modified particulate-$Cu_{0.8}Ag_{0.2}GaS_2$-based photocathode was dried at room temperature and sequentially was annealed at 473 or 773 K for 2 h in N_2 gas. These are denoted as ZnS(473)–CAGS and ZnS(773)–CAGS. Then, the ZnS-modified particulate-$Cu_{0.8}Ag_{0.2}GaS_2$-based photocathode with non-annealing is denoted as ZnS(NA)–CAGS. A $ZnSO_4$-adsorbed particulate-$Cu_{0.8}Ag_{0.2}GaS_2$-based photocathode was prepared by dipping the pristine photocathode into an aqueous solution dissolving only $ZnSO_4$, followed by annealing at 773 K for 2 h under a N_2 gas. The obtained sample is denoted as $ZnSO_4$(773)–CAGS. The $ZnSO_4$-adsorbed $Cu_{0.8}Ag_{0.2}GaS_2$ photocathode with non-annealing is denoted as $ZnSO_4$(NA)–CAGS. A CAGS photocathode was dipped into the mixture of thiourea, citric acid and an aqueous ammonia solution (namely, without $ZnSO_4$) and then was annealed at 773 K for 2 h under N_2 gas. The obtained sample is denoted as $ZnSO_4$-w/o-CAGS. If a $Cu_{0.8}Ag_{0.2}GaS_2$ photocathode was immersed in an aqueous solution containing either thiourea, citric acid or an aqueous ammonia solution followed by annealing at 773 K for 2 h, the obtained photoelectrodes are denoted as thiourea(773)–CAGS, citric acid(773)–CAGS and ammonia(773)–CAGS, respectively.

Cocatalysts were loaded on the surfaces of photocathodes. $AgNO_3$, $Cu(NO_3)_2$, $HAuCl_4$, H_2PtCl_6, $RuCl_3$ and $RhCl_3$ were employed as the cocatalyst sources. An aqueous solution containing either one of the cocatalyst sources was dripped on a photocathode. The amount of the loaded cocatalyst was 100 nmol cm^{-2}. After drying off the aqueous solvent at room temperature, the photocathode was annealed at 773 K for 2 h in N_2 gas. Since it has been reported that $RuCl_3$ loaded on the surface of the $Cu_{0.8}Ag_{0.2}GaS_2$ photocathode through annealing in N_2 gas is reduced to metallic Ru by cathodic photocurrent during photoelectrochemical H_2 formation in an aqueous solution,[9] various metal cocatalyst sources were loaded on the ZnS/$Cu_{0.8}Ag_{0.2}GaS_2$ photocathode through the same procedure as that of the literature[9] and could be reduced to the metallic state during the CO_2 reduction in our experiments. If necessary, the photocathode was immersed in a mixture of water and acetone (the ratio of 1 : 1 as volumes) for about 30 seconds

 This journal is © The Royal Society of Chemistry 2025

Open Access Article. Published on 27 January 2025. Downloaded on 2/13/2026 6:04:03 AM. This article is licensed under a Creative Commons Attribution-NonCommercial 3.0 Unported Licence.

Table 1 Control experiments for deposition of ZnS on particulate-$Cu_{0.8}Ag_{0.2}GaS_2$-based photocathodes[a]

		Conditions for ZnS deposition					
Entry	Sample notation	Citric acid	Ammonia	Thiourea	$ZnSO_4$	Anneal	Cathodic photocurrent density/μA cm^{-2}
1	CAGS	No	No	No	No	None	130
2	ZnS(NA)–CAGS	Yes	Yes	Yes	Yes	None	200
3	ZnS(473)–CAGS	Yes	Yes	Yes	Yes	473 K	650
4	ZnS(773)–CAGS	Yes	Yes	Yes	Yes	773 K	1850
5	Citric acid(773)–CAGS	Yes	No	No	No	773 K	130
6	Ammonia(773)–CAGS	No	Yes	No	No	773 K	200
7	Thiourea(773)–CAGS	No	No	Yes	No	773 K	13
8	$ZnSO_4$-w/o-CAGS	Yes	Yes	Yes	No	773 K	220
9	$ZnSO_4$(773)–CAGS	No	No	No	Yes	773 K	400

[a] Deposition time: 10 min. Photoelectrochemical measurement conditions; electrolyte: 0.1 mol L^{-1} of an aqueous K_2SO_4 solution with a phosphate buffer (pH 7) saturated with 1 atm of N_2 gas, light source: a 300 W Xe-arc lamp with a cut-off filter (λ > 420 nm), applied potential: 0 V *vs.* RHE.

before dropping the aqueous solution containing the cocatalyst source in order to remove its water-repellency. Photocathode samples were analyzed using an X-ray photoelectron spectrometer (JEOL; JSP-9010MC; Mg anode). The binding energies of X-ray photoelectron spectra were corrected with the C 1s (284.3 eV) contamination peak on metallic Au foil. The binding energy of the Au foil was corrected using the reference datum of Au foil (Au $4f_{7/2}$: 84.0 eV)[26] after a contamination and the oxide phase on the surface of the Au foil was carefully removed by Ar etching.

2.2 Photoelectrochemical measurement

Photoelectrochemical properties were evaluated using a potentiostat (Hokuto Denko; HSV-110). An H-type glass cell that consists of a working electrode cell and a counter electrode cell with a Nafion membrane (Dupont) to separate the compartment was used. A Pt wire and a saturated Ag/AgCl electrode (DKK-TOA) were used as counter and reference electrodes, respectively. 0.1 mol L^{-1} of $K_2SO_{4\ aq.}$ with a phosphate buffer (each 0.025 mol L^{-1} of $KH_2PO_{4\ aq.}$ and $Na_2HPO_{4\ aq.}$) (pH 7) and 0.1 mol L^{-1} of $KHCO_{3\ aq.}$ were employed as aqueous electrolytes, respectively. The electrolyte in the H-type glass cell was saturated with 1 atm of Ar, N_2 or CO_2 before measurements. pH of the aqueous $KHCO_3$ solution saturated with CO_2 was *ca.* 7. A 300 W Xe-arc lamp was employed as a light source. The wavelength of the irradiation light was controlled by a cut-off filter, an NIR-absorbing filter and band-pass filters. A solar simulator was employed as a light source of simulated sunlight (AM1.5G). The photocathode was irradiated with the light from the FTO side. The gaseous products were determined using gas chromatographs (Shimadzu; TCD, MS-5A, Ar and He carriers, detection of H_2 and O_2; FID with a methanizer, MS-13X, N_2 carrier, detection of CO). Formic acid was analyzed using an ion-chromatograph (TOSOH, IC-2000). An isotope experiment was conducted using $^{13}CO_2$ to confirm the carbon source of the product of the CO_2 reduction. ^{13}CO of the reduction product of $^{13}CO_2$ was analyzed using GC-MS (Shimadzu; GCMS-QP2010 Plus, RESTEK; RT-Msieve 5A). For photoelectrochemical measurement using a two-electrode-type cell, the photocathode (3.3 cm^2) was irradiated from the FTO side with the simulated sunlight through a photoanode (1.0 cm^2), resulting in that the total irradiation area was 3.3 cm^2.

3 Results and discussion

3.1 Surface modification with ZnS

Fig. 1 shows the effect of modification with ZnS on the photoelectrochemical properties of a particulate-$Cu_{0.8}Ag_{0.2}GaS_2$-based photocathode in an aqueous K_2SO_4 solution with a phosphate buffer (pH 7) saturated with 1 atm of N_2 gas under visible light irradiation. A pristine particulate-$Cu_{0.8}Ag_{0.2}GaS_2$-based photocathode gave a cathodic photocurrent under visible light irradiation as observed in a previous report (Fig. 1(a)).[9] The cathodic photocurrent was increased by modification with ZnS on the surface of the particulate-$Cu_{0.8}Ag_{0.2}GaS_2$-based photocathode by chemical bath deposition (CBD) (Fig. 1(b)). The onset potentials of the linear sweep voltammograms were affected by the difference in the CBD conditions (Fig. S1†), though it was difficult to find the relationship between the onset positions and the CBD conditions. Onsets of action spectra of the ZnS/$Cu_{0.8}Ag_{0.2}GaS_2$ photocathodes almost agreed with the absorption edge of pristine $Cu_{0.8}Ag_{0.2}GaS_2$ powder (Fig. 2), indicating that the cathodic photocurrent was generated by the

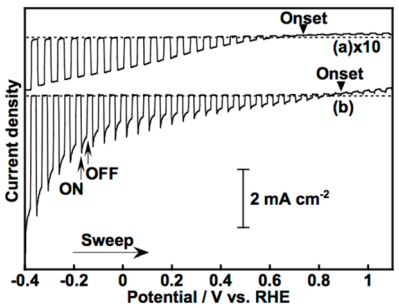

Fig. 1 Linear sweep voltammograms of (a) pristine and (b) ZnS-modified particulate-$Cu_{0.8}Ag_{0.2}GaS_2$-based photocathodes under visible light irradiation. Electrolyte: 0.1 mol L^{-1} of an aqueous K_2SO_4 solution with a phosphate buffer (pH 7) saturated with 1 atm of N_2 gas, light source: a 300 W Xe-arc lamp with a cut-off filter (λ > 420 nm).

Open Access Article. Published on 27 January 2025. Downloaded on 2/13/2026 6:04:03 AM.
This article is licensed under a Creative Commons Attribution-NonCommercial 3.0 Unported Licence.

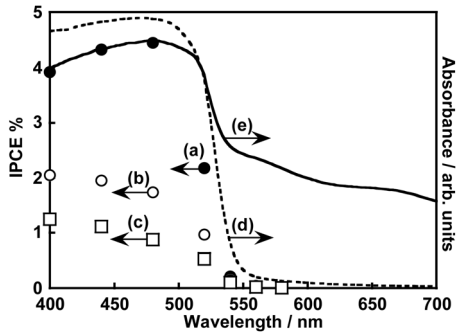

Fig. 2 Action spectra of ZnS/$Cu_{0.8}Ag_{0.2}GaS_2$ photocathodes at (a) −0.4, (b) 0 and (c) 0.3 V *vs.* RHE and diffuse reflectance spectra of (d) pristine $Cu_{0.8}Ag_{0.2}GaS_2$ powder and (e) the ZnS/$Cu_{0.8}Ag_{0.2}GaS_2$ photocathode. Electrolyte: 0.1 mol L^{-1} of an aqueous K_2SO_4 solution with a phosphate buffer (pH 7) saturated with 1 atm of N_2 gas, light source: a 300 W Xe-arc lamp with band-pass filters.

band gap excitation of $Cu_{0.8}Ag_{0.2}GaS_2$. Fig. 3 shows the time course of the photoelectrochemical H_2 formation using the ZnS/$Cu_{0.8}Ag_{0.2}GaS_2$ photocathode. Although the photocurrent density was fairly high in the initial period (Fig. 3(a)), the value decreased with reaction time (Fig. 3(b)). This deactivation in the initial period could be attributed to the elution of the ZnS similar to the CdS deposited on chalcogenide photocathodes.[12,27,28] The observed photocurrent of the ZnS/$Cu_{0.8}Ag_{0.2}GaS_2$ in the later period almost corresponded to the H_2 evolution rates under visible light, indicating that the faradaic efficiency was almost 100% (Fig. 3(b)). In order to clarify the experimental factor affecting the H_2 formation rate over a ZnS-modified $Cu_{0.8}Ag_{0.2}GaS_2$ photocathode, control experiments were performed (Table 1). The annealing procedure after the ZnS modification with CBD was effective in improving the photocurrent density, while the photocurrent density of the pristine one was slightly enhanced by ZnS modification without annealing (Table 1, entries 1–4). Among them, annealing at 773 K was the most effective here. This is because, considering the heat resistance of FTO glass substrates, 773 K is close to the limit temperature. In contrast, significant improvement was not observed in the absence of $ZnSO_4$ in the starting materials for CBD with annealing at 773 K (Table 1, entries 5–8). The photocurrent density of a $ZnSO_4$-modified $Cu_{0.8}Ag_{0.2}GaS_2$ photocathode was larger than that of the pristine one (Table 1, entry 9). Thus, the cathodic photocurrent of $Cu_{0.8}Ag_{0.2}GaS_2$ was significantly improved when all of $ZnSO_4$, thiourea, citric acid and ammonia were used for CDB with annealing at 773 K.

The surface configuration of the ZnS/$Cu_{0.8}Ag_{0.2}GaS_2$ photocathode was examined using X-ray photoelectron spectra (XPS), Auger spectra and additional control experiments. Auger spectra indicated that the deposited ZnS partly included ZnO and $Zn(OH)_2$ (Fig. S2†). The ZnO and $Zn(OH)_2$ still existed at the surface even after annealing at 473 K. Such auger spectra disappeared after annealing at 773 K. Moreover, intensities of Zn 2p XPS peaks decreased with the increase in the annealing temperature, and annealing at 773 K drastically decreased the intensities (Fig. S3†). These auger and XPS measurements indicated the following two points; (i) deposited ZnS including ZnO and $Zn(OH)_2$ existed at the surface of ZnS(473)–CAGS, (ii) deposited Zn species were diffused in the surface of $Cu_{0.8}Ag_{0.2}GaS_2$ particles in ZnS(773)–CAGS. In other words, an annealing at 773 K is crucial to diffuse the ZnS deposited on the $Cu_{0.8}Ag_{0.2}GaS_2$ particles into the neighbourhood in the surface of the $Cu_{0.8}Ag_{0.2}GaS_2$ particles as summarized in Fig. 4(A). Specifically, the surface of the $Cu_{0.8}Ag_{0.2}GaS_2$ particles was covered with ZnS either of particles or film (Fig. 4(A)(a) and (b)). Afterwards, the ZnS was diffused into the $Cu_{0.8}Ag_{0.2}GaS_2$ particles by annealing at 773 K, though almost all of the ZnS existed in the neighbourhood in the surface (Fig. 4(A)(c)). This diffusion made the solid-solution of (ZnS)–($Cu_{0.8}Ag_{0.2}GaS_2$) in the neighbourhood in the surface. The concentration of the diffused ZnS was gradually diluted from the surface to the bulk. Therefore, a crucial factor of the improvement was formation of

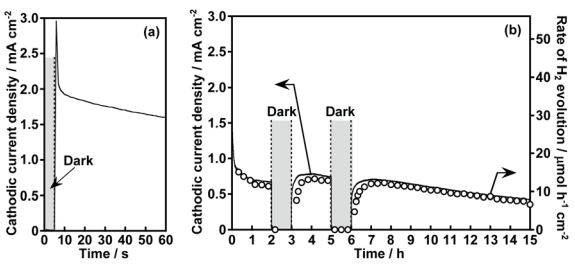

Fig. 3 Photoelectrochemical H_2 evolution using a ZnS/$Cu_{0.8}Ag_{0.2}GaS_2$ photocathode under visible light irradiation in (a) the initial and (b) the whole period of the reaction time. Electrolyte: 0.1 mol L^{-1} of an aqueous K_2SO_4 solution with a phosphate buffer (pH 7) saturated with 1 atm of Ar gas, light source: a 300 W Xe-arc lamp with a cut-off filter (λ > 420 nm), applied potential: 0 V *vs.* RHE.

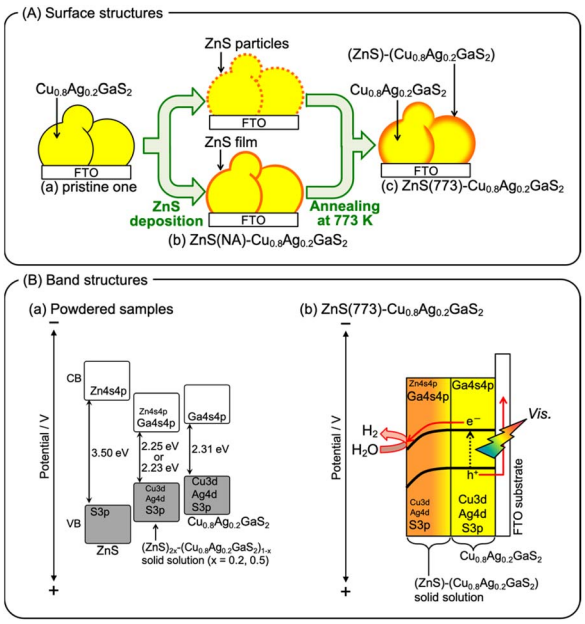

Fig. 4 (A) Proposed surface structures of the particulate-$Cu_{0.8}Ag_{0.2}GaS_2$-based photocathode, and (B) proposed band structures of $(ZnS)_{2x}$–$(Cu_{0.8}Ag_{0.2}GaS_2)_x$ powders and the ZnS(773)–$Cu_{0.8}Ag_{0.2}GaS_2$ photocathode. The band gaps were estimated from the adsorption edges shown in Fig. S4.†

 This journal is © The Royal Society of Chemistry 2025

Open Access Article. Published on 27 January 2025. Downloaded on 2/13/2026 6:04:03 AM. This article is licensed under a Creative Commons Attribution-NonCommercial 3.0 Unported Licence.

the (ZnS)–($Cu_{0.8}Ag_{0.2}GaS_2$) solid-solution in the neighbourhood in the particulate $Cu_{0.8}Ag_{0.2}GaS_2$ surface. This crucial factor could provide the following effects. The surface incorporated with ZnS could work as an active site for photoelectrochemical water reduction, since ZnS is a well-known active photocatalyst for H_2 formation without loading of cocatalysts.[29–32] Another aspect of the improvement may lie in the gradient of the band structure as shown in Fig. 4(B). The band gap of powdered $Cu_{0.8}Ag_{0.2}GaS_2$ was narrowed by forming the solid-solution of powdered (ZnS)–($Cu_{0.8}Ag_{0.2}GaS_2$) (Fig. S4†). The same phenomenon to narrow the band gaps by homogeneously mixing with ZnS has been reported in the case of the (ZnS)–($CuGaS_2$) solid-solution (namely, no Ag constituent).[33] These narrowed band gaps could be explained by the increase in the symmetries of MS_4 tetrahedrons (M = Zn, Cu, and Ga), implying that the conduction band minimum and valence band maximum both are shifted downwardly.[33] Again, XRD spectra of the (ZnS)–($Cu_{0.8}Ag_{0.2}GaS_2$) (Fig. S4†) show that the MS_4 tetrahedrons (M = Zn, Cu, Ag, and Ga) tended to be close to the symmetrical tetrahedrons, judging from the peak splitting. Therefore, the conduction band minimum and valence band maximum of powdered (ZnS)–($Cu_{0.8}Ag_{0.2}GaS_2$) might be located at more positive potentials than those of $Cu_{0.8}Ag_{0.2}GaS_2$ (Fig. 4(B)(a)). As for the structural information, no morphological changes in a series of ZnS-modified $Cu_{0.8}Ag_{0.2}GaS_2$ were observed using a scanning electron microscope (SEM), though it was difficult to clarify the structural configurations of the deposited ZnS in the observations using a SEM equipped with an energy dispersive X-ray spectrometer (SEM-EDS) (Fig. S5†). Although the quantitative consistency of the ZnS ratios between the photocathode and the powders was unclear, the aforementioned effect to alter the band positions implied that the conduction band minimum and valence band maximum of the neighbourhood in the surface gradually shifted downwardly due to the concentration gradient of the solid-solution of ZnS(773)–$Cu_{0.8}Ag_{0.2}GaS_2$ (Fig. 4(B)(b)). Assuming that the absorption coefficient of (ZnS)–($Cu_{0.8}Ag_{0.2}GaS_2$) is similar to that of $CuGaS_2$ in the visible light region (20 000–50 000 cm^{-1}),[34] the ZnS-modified $Cu_{0.8}Ag_{0.2}GaS_2$ particles near FTO were mainly photoexcited. This is because the transmittance of incident photons would be at least 0.01% when the diameters of ZnS(773)-modified $Cu_{0.8}Ag_{0.2}GaS_2$ particles were *ca.* 2 μm (Fig. S5†). Indeed, we reported that $CuGaS_2$ particles being far from FTO have little contribution to the photocurrents of particulate-$CuGaS_2$-based photocathodes.[35,36] Finally, the photogenerated electrons migrated to the surface region by the band bending of the ZnS-modified $Cu_{0.8}Ag_{0.2}GaS_2$ particles, resulting in enhancement of the separation of the photogenerated carriers (Fig. 4(B)(b)). These two aspects could be the crucial factors for the improvement by the ZnS modification.

3.2 Effect of cocatalysts loaded over ZnS/$Cu_{0.8}Ag_{0.2}GaS_2$ photocathodes on CO_2 reduction performances

Table 2 shows the application of the ZnS(773)–$Cu_{0.8}Ag_{0.2}GaS_2$ photocathode (denoted as ZnS/$Cu_{0.8}Ag_{0.2}GaS_2$, hereafter) to CO_2 reduction under visible light and the effects of additional modification of ZnS/$Cu_{0.8}Ag_{0.2}GaS_2$ photocathodes with various cocatalysts. In this measurement, an aqueous $KHCO_3$ solution saturated with 1 atm of CO_2 gas (pH was *ca.* 7) was used as an electrolyte and 0 V *vs.* RHE was constantly applied to the photocathodes. Again, the pristine particulate-$Cu_{0.8}Ag_{0.2}GaS_2$-based photocathode gave a cathodic photocurrent in the aqueous $KHCO_3$ electrolyte (Table 2, entry 1). Partial cathodic photocurrent densities ($J_{partial}$) for H_2 and CO formations were certainly estimated. The surface modification with ZnS was effective for improving both $J_{partial}$ and FE_{CO} (Table 2, entry 2). Considering the literature about photoelectrochemical CO_2 reduction to form CO over surfaces of $(CuGa)_{0.5}ZnS_2$ (ref. 10) and ZnS-modified Cu_2ZnGeS_4 (ref. 13) photocathodes, the surface of ZnS/$Cu_{0.8}Ag_{0.2}GaS_2$ seems to be effective for CO formation. No cathodic photocurrents for H_2 and CO formation were observed under darkness (Table 2, entry 3). In an aqueous K_2SO_4 solution with a phosphate buffer (pH 7) saturated with 1 atm of N_2 gas under visible light irradiation instead of the $KHCO_3$ electrolyte, photocurrent density only for H_2 formation was observed (Table 2, entry 4). Various cocatalysts were further loaded on the surfaces of the ZnS/$Cu_{0.8}Ag_{0.2}GaS_2$ photocathodes (Table 2, entries 5–13). Noble metal cocatalysts of Pt, Rh and Ru were not effective for CO_2 reduction (Table 2, entries 5–7). Although the faradaic efficiencies of Pt- and Ru-loaded ones were beyond 100%, this is most likely because of experimental errors associated with usage of a syringe (1 mL) to extract the gaseous products. Au, Cu and Ag cocatalysts improved the partial current densities not only for H_2 formation but also for CO formation (Table 2, entries 8–10). The Ag-loaded ZnS/$Cu_{0.8}Ag_{0.2}GaS_2$ (Ag/ZnS/$Cu_{0.8}Ag_{0.2}GaS_2$) photocathode showed the highest partial cathodic photocurrent densities for H_2 and CO formation. This sufficient performance was only obtained when the surface was modified with both ZnS and Ag accompanied by annealing (Table 2, entries 10–13). Considering the following three insights: (1) $RuCl_3$ loaded on the surface of the $Cu_{0.8}Ag_{0.2}GaS_2$ photocathode through annealing in N_2 gas is reduced to metallic Ru by cathodic photocurrent during photoelectrochemical H_2 formation in an aqueous solution,[9] (2) In_2S_3 modified on a Cu_2ZnSnS_4 photocathode is reduced to metallic In during the photoelectrochemical reduction reaction,[12] (3) powdered Ag-containing metal sulfide photocatalysts with high apparent quantum yield for H_2 formation may reduce silver sulfide to metallic Ag during H_2 formation in an aqueous solution,[37,38] it was suggested that the cathodic photocurrent was partly used to reduce the silver species loaded on the surface to metallic silver at the beginning stage. This metallic silver could be electrochemically active for CO_2 reduction as reported in the literature about an Ag metal electrode.[39,40] The bubbles mixed with H_2 and CO gases were visually generated on the Ag/ZnS/$Cu_{0.8}Ag_{0.2}GaS_2$ photocathode accompanied by O_2 production on a Pt counter electrode when 0 V *vs.* RHE was applied to the photocathode under visible light irradiation (see an attached movie file). The Ag/ZnS/$Cu_{0.8}Ag_{0.2}GaS_2$ photocathode was active even under simulated sunlight (Fig. 5). An isotope experiment using $^{13}CO_2$ was conducted to confirm the carbon source of CO obtained. An aqueous K_2SO_4 solution saturated with 1 atm of $^{13}CO_2$ was employed as the electrolyte

Open Access Article. Published on 27 January 2025. Downloaded on 2/13/2026 6:04:03 AM.
This article is licensed under a Creative Commons Attribution-NonCommercial 3.0 Unported Licence.

Table 2 Effects of various surface modifications of particulate $Cu_{0.8}Ag_{0.2}GaS_2$-based photocathodes on photoelectrochemical CO_2 reduction under visible light[a]

						$J_{partial}$/μA cm^{-2}			
Entry	Cocatalyst	Annealing[b]	ZnS	Light	Gas	H_2	CO	FE_{CO} %	FE_{Total} %
1	None	—	No	Yes	CO_2	10	0.3	3	98
2	None	—	Yes	Yes	CO_2	430	70	14	95
3	None	—	Yes	No	CO_2	0	0	—	—
4	None	—	Yes	Yes	N_2	1200	0	0	97
5	Pt	773 K	Yes	Yes	CO_2	790	10	1	117
6	Rh	773 K	Yes	Yes	CO_2	420	30	7	100
7	Ru	773 K	Yes	Yes	CO_2	90	5	5	127
8	Au	773 K	Yes	Yes	CO_2	890	200	17	100
9	Cu	773 K	Yes	Yes	CO_2	620	200	24	92
10	Ag	773 K	Yes	Yes	CO_2	1600	330	17	100
11	Ag	773 K	No	Yes	CO_2	190	5	3	96
12	Ag	None	No	Yes	CO_2	60	1	2	98
13	Ag	None	Yes	Yes	CO_2	130	7	5	91

[a] Electrolyte: 0.1 mol L^{-1} of an aqueous $KHCO_3$ solution saturated with 1 atm of CO_2 gas (pH was *ca.* 7), light source: a 300 W Xe-arc lamp with a cut-off filter ($\lambda > 420$ nm), applied potential: 0 V *vs.* RHE, reactor: a closed H-type glass cell (namely, a batch-type reactor). $J_{partial}$ indicates an average of a partial cathodic photocurrent density for 3 h. For quantification of the gaseous products, a syringe (1 mL) was used to extract the gas. [b] Annealing was performed under a N_2 atmosphere for loading cocatalysts. FE_{CO} = (sum of the number of electrons consumed for CO formation)/(sum of the number of electrons passing through the outer circuit) × 100. FE_{total} = (sum of the number of electrons consumed for H_2 and CO formation)/(sum of the number of electrons passing through the outer circuit) × 100.

(Fig. S6†). Not ^{12}CO but ^{13}CO was obtained as the reduction product of $^{13}CO_2$ over the $Ag/ZnS/Cu_{0.8}Ag_{0.2}GaS_2$ photocathode, indicating that the carbon source of the obtained CO was a CO_2 molecule. When Ag, Cu and Au cocatalysts were employed, a small amount of formic acid was detected but it was difficult to quantify the formic acid. Thus, co-modification with ZnS and Ag using annealing has arisen as a new effective technique for improving the performance of the particulate-$Cu_{0.8}Ag_{0.2}GaS_2$-based photocathode for the CO_2 reduction to form CO accompanied by H_2 formation in an aqueous solution under simulated sunlight.

3.3 Photoelectrochemical syngas formation using water as an electron doner under simulated sunlight

Fig. 6 shows CO_2 reduction using a photoelectrochemical cell consisting of a $Ag/ZnS/Cu_{0.8}Ag_{0.2}GaS_2$ photocathode and a $CoO_x/BiVO_4$ photoanode[41] in an aqueous $KHCO_3$ solution saturated with 1 atm of CO_2 gas. This photoelectrochemical cell of which the structure was partly a tandem-type gave photocurrent under simulated sunlight irradiation without any external bias. This is due to an overlap between onset potentials of the photocathode and the photoanode in the CO_2-saturated $KHCO_3$ electrolyte, as shown in Fig. 7. Considering that the

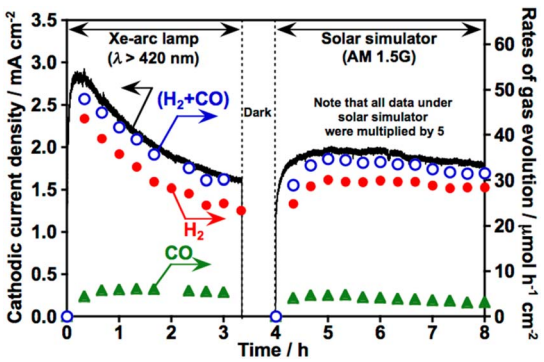

Fig. 5 Photoelectrochemical CO_2 reduction using the $Ag/ZnS/Cu_{0.8}Ag_{0.2}GaS_2$ photocathode under visible light and simulated sunlight irradiation. Electrolyte: 0.1 mol L^{-1} of an aqueous $KHCO_3$ solution saturated with 1 atm of CO_2 gas, light source: a 300 W Xe-arc lamp with a cut-off filter ($\lambda > 420$ nm) and a solar simulator (AM1.5G), applied potential: 0 V *vs.* RHE. All of the observed current and the production rates under simulated solar light were multiplied by 5 for ease of the discussion of the performances.

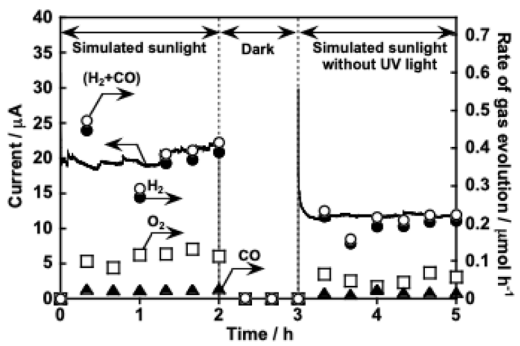

Fig. 6 CO_2 reduction utilizing water as an electron donor using a photoelectrochemical cell consisting of an $Ag/ZnS/Cu_{0.8}Ag_{0.2}GaS_2$ photocathode and a $CoO_x/BiVO_4$ photoanode under simulated sunlight without any external bias. Electrolyte: 0.1 mol L^{-1} of an aqueous $KHCO_3$ solution saturated with 1 atm of a CO_2 gas, light source: a solar simulator (AM1.5G) without/with a cut-off filter ($\lambda > 420$ nm), area of electrodes: $Ag/ZnS/Cu_{0.8}Ag_{0.2}GaS_2$ photocathode; 3.3 cm^2 and $CoO_x/BiVO_4$ photoanode; 1.0 cm^2.

 This journal is © The Royal Society of Chemistry 2025

Open Access Article. Published on 27 January 2025. Downloaded on 2/13/2026 6:04:03 AM.
This article is licensed under a Creative Commons Attribution-NonCommercial 3.0 Unported Licence.

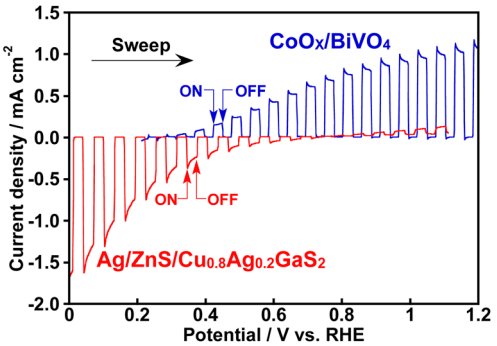

Fig. 7 Linear sweep voltammograms of an Ag/ZnS/$Cu_{0.8}Ag_{0.2}GaS_2$ photocathode and a $CoO_x/BiVO_4$ photoanode under visible light irradiation. Electrolyte: in 0.1 mol L^{-1} of an aqueous $KHCO_3$ solution saturated with 1 atm of a CO_2 gas, light source: a 300 W Xe-arc lamp with a cut-off filter (λ > 420 nm).

absorption coefficient of $BiVO_4$ at 420 nm is 67 000 cm^{-1},[42] 1% of the incident photons could arrive at the Ag/ZnS/$Cu_{0.8}Ag_{0.2}GaS_2$ photocathode when the thickness of our $BiVO_4$ was regarded to be similar to the literature (*ca.* 300 nm).[41] The faradaic efficiency for CO formation using the Ag/ZnS/$Cu_{0.8}Ag_{0.2}GaS_2$ photocathode was *ca.* 20% regardless of the decrease in the incident photons and change in the applied potentials (Table S1†). Therefore, the cell of which the structure was partly a tandem-type would hardly affect the selectivity for syngas formation. By paying attention to Fig. 6 again, observed photocurrent almost corresponded to the summation of CO and H_2 formation in the cathode cell, indicating that the photocurrent was used for syngas formation through photoelectrochemical reduction of water and CO_2. Most importantly, O_2 of the oxidation product of water was certainly obtained in the anode cell, whereas the rate of O_2 formation was slightly less than the stoichiometry due to an experimental error with the lower photocurrent. The photocurrent was continuously observed even under visible light included in simulated sunlight without any external bias. This indicated that this cell possessed an ability to utilize the visible light of sunlight. Thus, we successfully demonstrated solar syngas formation through the reduction of water and CO_2 separately from O_2 of the oxidation product of water upon constructing the photoelectrochemical cell consisting of the developed Ag/ZnS/$Cu_{0.8}Ag_{0.2}GaS_2$ photocathode and the $CoO_x/BiVO_4$ photoanode.

4 Conclusions

A co-modification with ZnS and Ag has been developed for improvement in H_2O and CO_2 reduction over a particulate-$Cu_{0.8}Ag_{0.2}GaS_2$-based photocathode to form H_2 and CO under visible light in an aqueous electrolyte. The faradaic efficiency and the partial cathodic photocurrent density for CO formation over the Ag/ZnS/$Cu_{0.8}Ag_{0.2}GaS_2$ photocathode achieved approximately 20% and 300 μA cm^{-2}, respectively, at 0 V *vs.* RHE. The Ag/ZnS/$Cu_{0.8}Ag_{0.2}GaS_2$ photocathode was successfully combined with a $CoO_x/BiVO_4$ photoanode for constructing a photoelectrochemical cell. This photoelectrochemical cell gave steady photocurrent under simulated sunlight irradiation without any external bias, resulting in syngas (H_2 and CO) formation using water as an electron donor. The knowledge in this work is expected to contribute to development of new particulate-photocatalyst-based photocathodes for highly efficient syngas production under sunlight.

Data availability

The data supporting this article have been included as ESI.†

Conflicts of interest

There are no conflicts to declare.

Acknowledgements

This work was supported by a Grant-in-Aid for Scientific Research (MEXT KAKENHI Grant Number: 17H06440, 17H06433 and 23H00248) and Grant-in-Aid for Young Scientists (B) (16K17948) from the Ministry of Education, Culture, Sports, Science and Technology in Japan.

Notes and references

1 T. Hisatomi, J. Kubota and K. Domen, *Chem. Soc. Rev.*, 2014, **43**, 7520.
2 H. Kaneko, T. Minegishi and K. Domen, *Chem.–Eur. J.*, 2018, **24**, 5697.
3 J. L. White, M. F. Baruch, J. E. Pander III, Y. Hu, I. C. Fortmeyer, J. E. Park, T. Zhang, K. Liao, J. Gu, Y. Yan, T. W. Shaw, E. Abelev and A. B. Bocarsly, *Chem. Rev.*, 2015, **115**, 12888.
4 A. Dey, D. Maiti and G. K. Lahiri, *Asian J. Org. Chem.*, 2017, **6**, 1519.
5 V. Kumaravel, J. Bartlett and S. C. Pillai, *ACS Energy Lett.*, 2020, **5**, 486.
6 W. Zhou, K. Cheng, J. Kang, C. Zhou, V. Subramanian, Q. Zhan and Y. Wang, *Chem. Soc. Rev.*, 2019, **48**, 3193.
7 T. Morikawa, S. Sato, K. Sekizawa, T. M. Suzuki and T. Arai, *Acc. Chem. Res.*, 2022, **55**, 933.
8 W. Septina, Gunawan, S. Ikeda, T. Harada, M. Higashi, R. Abe and M. Matsumura, *J. Phys. Chem. C*, 2015, **119**, 8576.
9 H. Kaga, Y. Tsutsui, A. Nagane, A. Iwase and A. Kudo, *J. Mater. Chem. A*, 2015, **3**, 21815.
10 S. Yoshino, A. Iwase, Y. Yamaguchi, T. M. Suzuki, T. Morikawa and A. Kudo, *J. Am. Chem. Soc.*, 2022, **144**, 2323.
11 T. Arai, S. Tajima, S. Sato, K. Uemura, T. Morikawa and T. Kajino, *Chem. Commun.*, 2011, **47**, 12664.
12 S. Kamimura, Y. Sasaki, M. Kanaya, T. Tsubota and T. Ohno, *RSC Adv.*, 2016, **6**, 112594.
13 S. Ikeda, S. Fujikawa, T. Harada, H. T. Nguyen, S. Nakanishi, T. Takayama, A. Iwase and A. Kudo, *ACS Appl. Energy Mater.*, 2019, **2**, 6911.
14 T. Takashima, Y. Fujishiro and H. Irie, *Catalysts*, 2020, **10**, 949.

Open Access Article. Published on 27 January 2025. Downloaded on 2/13/2026 6:04:03 AM.
This article is licensed under a Creative Commons Attribution-NonCommercial 3.0 Unported Licence.

15 P. B. Pati, R. Wang, E. Boutin, S. Diring, S. Jobic, N. Barreau, F. Odobel and M. Robert, *Nat. Commun.*, 2020, **11**, 3499.
16 S. Sato, T. Arai, T. Morikawa, K. Uemura, T. M. Suzuki, H. Tanaka and T. Kajino, *J. Am. Chem. Soc.*, 2011, **133**, 15240.
17 T. Arai, S. Sato, T. Kajino and T. Morikawa, *Energy Environ. Sci.*, 2013, **6**, 1274.
18 Y. J. Jang, I. Jeong, J. Lee, J. Lee, M. J. Ko and J. S. Lee, *ACS Nano*, 2016, **10**, 6980.
19 R. Hinogami, Y. Nakamura, S. Yae and Y. Nakato, *J. Phys. Chem. B*, 1998, **102**, 974.
20 S. Roy, M. Miller, J. Warnan, J. J. Leung, C. D. Sahm and E. Reisner, *ACS Catal.*, 2021, **11**, 1868.
21 J. Gu, A. Wuttig, J. W. Krizan, Y. Hu, Z. M. Detweiler, R. J. Cava and A. B. Bocarsly, *J. Phys. Chem. C*, 2013, **117**, 12415.
22 M. Xia, L. Pan, Y. Liu, J. Gao, J. Li, M. Mensi, K. Sivula, S. M. Zakeeruddin, D. Ren and M. Grätzel, *J. Am. Chem. Soc.*, 2023, **145**, 27939.
23 H. Kumagai, G. Sahara, K. Maeda, M. Higashi, R. Abe and O. Ishitani, *Chem. Sci.*, 2017, **8**, 4242.
24 K. Sekizawa, S. Sato, T. Arai and T. Morikawa, *ACS Catal.*, 2018, **8**, 1405.
25 W. L. Liu, C. S. Yang, S. H. Hsieh, W. J. Chen and C. L. Fern, *Appl. Surf. Sci.*, 2013, **264**, 213.
26 M. P. Seah, *Surf. Interface Anal.*, 1989, **14**, 488.
27 L. Zhang, T. Minegishi, J. Kubota and K. Domen, *Phys. Chem. Chem. Phys.*, 2014, **16**, 6167.
28 J. Zhao, T. Minegishi, L. Zhang, M. Zhong, M. Gunawan, M. Nakabayashi, G. Ma, T. Hisatomi, M. Katayama, S. Ikeda, N. Shibata, T. Yamada and K. Domen, *Angew. Chem., Int. Ed.*, 2014, **53**, 11808.
29 S. Yanagida, T. Azuma and H. Sakurai, *Chem. Lett.*, 1982, 1069.
30 J.-F. Reber and K. Meier, *J. Phys. Chem.*, 1984, **88**, 5903.
31 N. Zeug, J. Bücheler and H. Kisch, *J. Am. Chem. Soc.*, 1985, **107**, 1459.
32 H. Kisch and J. Bücheler, *Bull. Chem. Soc. Jpn.*, 1990, **63**, 2378.
33 T. Kato, Y. Hakari, S. Ikeda, Q. Jia, A. Iwase and K. Kudo, *J. Phys. Chem. Lett.*, 2015, **6**, 1042.
34 R. Long, N. J. English and O. V. Prezhdo, *J. Am. Chem. Soc.*, 2012, **134**, 14238.
35 A. Iwase, Y. H. Ng, R. Amal and A. Kudo, *J. Mater. Chem. A*, 2015, **3**, 8566.
36 T. Takayama, A. Iwase and A. Kudo, *ACS Appl. Mater. Interfaces*, 2024, **16**, 36423.
37 I. Tsuji, Y. Shimodaira, H. Kato, H. Kobayashi and A. Kudo, *Chem. Mater.*, 2010, **22**, 1402.
38 H. Kaga, K. Saito and A. Kudo, *Chem. Commun.*, 2010, **46**, 3779.
39 Y. Hori, H. Wakebe, T. Tsukamoto and O. Koga, *Electrochim. Acta*, 1994, **39**, 1833.
40 T. Hatsukade, K. P. Kuhl, E. R. Cave, D. N. Abram and T. F. Jaramillo, *Phys. Chem. Chem. Phys.*, 2014, **16**, 13814.
41 Q. Jia, K. Iwashina and A. Kudo, *Proc. Natl. Acad. Sci. U. S. A.*, 2012, **109**, 11564.
42 I. Grigioni, A. Polo, M. V. Dozzi, K. G. Stamplecoskie, D. H. Jara, P. V. Kamat and E. Selli, *ACS Appl. Energy Mater.*, 2022, **5**, 13142.

 This journal is © The Royal Society of Chemistry 2025